

Mutual Coupling Reduction of Dual-Band Uni-Planar MIMO System Using Neutralization Line Technique

Adham M. Saleh^{1,2}, Tariq A. Nagim², Raed A. Abd-Alhameed¹, James M. Noras¹,
and Chan H. See³

¹School of Electrical Engineering and Computer Science
University of Bradford, Bradford, BD7 1DP, UK
amssaleh@bradford.ac.uk, r.a.a.abd@bradford.ac.uk, j.m.noras@bradford.ac.uk

²College of Electronic Engineering
Ninevah University, Mosul, Iraq
tanalniemi@gmail.com

³School of Engineering and the Built Environment
Edinburgh Napier University, Edinburgh, EH14 1DJ
C.See@napier.ac.uk

Abstract — This paper presents a low-profile dual-band (2×2) MIMO antenna that works at 2.4GHz, 5.2GHz and 5.8GHz for wireless local area networks (WLAN) applications. A neutralization line technique for enhancing the isolation is used by introducing a strip line with a length of $\lambda_g/4$ at the isolation frequency (2.4GHz) between the radiating elements. The overall dimensions of the proposed antenna are 36×33.5×1.6 mm³. The antenna is fabricated and tested to validate the simulation results. The practical results show fair agreements with the simulated outcomes. The antenna achieves impedance bandwidths from 2.15GHz to 2.52GHz and from 4.5GHz to 6.45GHz for reflection coefficient $|S_{11}| < -10\text{dB}$. On the other hand, the result of S_{21} for the two bands is better than -10dB and it has reached to -25dB around 2.4GHz and -35dB around 5.5GHz. The MIMO antenna performance characteristics are reported in terms of scattering parameters, envelope correlation coefficient (ECC), total active reflection coefficient (TARC), channel capacity loss (CCL), diversity gain (DG) and antenna radiation patterns. Analysis of these characteristics indicates that the design is appropriate for the WLAN.

Index Terms — MIMO antenna, mutual coupling, parasitic elements, WLAN.

I. INTRODUCTION

Recently, the wireless communications systems are expanded explosively to support the increasing demands of high transmission rate with high throughput for various fixed and mobile services. To fulfil these demands, the researchers and the manufacturers shifted from one antenna to multiple antenna systems. Multiple Input

Multiple Output (MIMO) system can be considered as the backbone of the new wireless technologies due to its unique features of achieving higher data rates without consuming extra power in the multipath environment [1, 2]. One significant drawback associated with the MIMO system is the mutual coupling between the radiating elements inside the MIMO antenna structure. This means that some of the energy will be radiated from one element to the other one and vice versa. The main reason for this issue is the close placement of the multiple radiating elements inside the MIMO antenna structure. As a result, if the radiating elements are closer, the coupling between them will be stronger [3, 4].

Various techniques were developed in the last few years to enhance the isolation inside the MIMO antenna structure. Various antenna designs with different band classifications such as narrowband, wideband and dual/triple band have used these approaches [5]. Methods reported include using parasitic elements between the antennas [6, 7], junctions and branches in the form of T-shape [8, 9], defected ground structures (DGS) [10, 11], stubs [11, 12], neutralization lines (NL) [13-17] and metamaterial resonators [18-25].

The neutralization line technique can be classified as one of the effective methods that are used to improve the isolation in MIMO antenna systems as illustrated in [13-17]. According to Chebihi *et al.* in [26], the main function of the NL is to pass the electromagnetic (EM) wave from one radiating element to the other one at a certain point inside the MIMO antenna structure via a metallic slit or lumped element. This EM wave should have an opposite coupling to reduce the main coupling in the antenna system at a specific frequency band [27].

The critical issue associated with this technique is the selection of the point. The position of the point inside the radiating structure should have low impedance and high current density [28]. Two parameters should be taken into account in the designing of NL; the first parameter is the length and the second one is the width. These parameters have a great effect on the results of the mutual coupling. Recently, the neutralization line technique was explained by several mobile phone companies. For example, Samsung [29] and LG Electronics [30] as a very effective mechanism for solving isolation problems in MIMO antenna systems. Several types of neutralization line structures are used in literature such as thin printed neutralization lines [31], pair of crossed neutralization lines [32], LC matching network and NL [33] and neutralization lines between ground planes [34].

In this paper, a low profile dual-band MIMO antenna is proposed to cover the WLAN bands (2.4/5.2/5.8GHz). The designed antenna basically consists of two uni-planar double T-shaped monopole antennas. A neutralization lines technique is used to connect the two radiating elements of the proposed MIMO antenna. The main aim of this paper is to optimize the NL positions and widths to validate the effectiveness of the NL on the isolation and the impedance bandwidth of the proposed antenna. The proposed antenna is fabricated to validate the simulation results. The antenna performance characteristics are reported in terms of scattering parameters, ECC, TARC, CCL, DG and antenna radiation patterns. Analysis of these characteristics indicates that the design is appropriate for WLAN applications.

II. ANTENNA DESIGN

In this design, a dual-band MIMO antenna with two double T-shaped radiating elements is modelled and simulated to fulfil the requirements of WLAN applications. FR4 with 1.6mm thickness, 4.3 relative permittivity, and 0.025 tangent loss is used as a substrate material for the proposed design of size $36 \times 33.5 \times 1.6$ mm³. The inter-element distance between the radiators is kept at $0.024\lambda_0$, which is equivalent to 3mm. on the other hand, the centre to centre separation is kept at 16.5mm. The antennas share the same ground plane in the bottom layer of the substrate. The ground plane is beveled to prevent proximity effects. Initially, a simple two double T-shaped radiating elements are modelled to work at dual frequency bands. The simple approach to design an antenna with a dual-band operation is by obtaining two elements with different lengths inside the antenna structure. So that, each element will resonate at the desired frequency by matching its length with a quarter of the wavelength of the operating frequency [35]. Therefore, the upper-frequency band is controlled by the shorter T-shaped arm while the lower frequency band is controlled by the longer T-shaped arm. Moreover,

a neutralization line with a length of 16.5mm is constructed to connect the two radiating elements for isolation enhancement purposes. The length of the NL is equivalent to $\lambda_g/4$ at the isolation frequency (2.4GHz). The schematic structure of the proposed antenna is shown in Fig. 1 and all the optimized dimensions are summarized in Table 1.

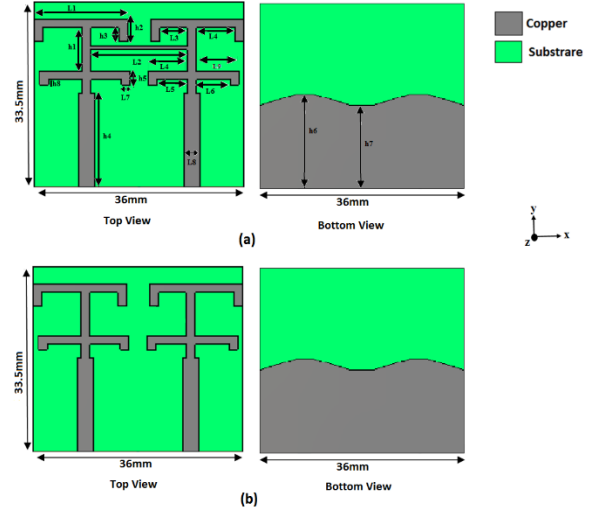


Fig. 1. The configuration of the proposed antenna: (a) antenna with NL, and (b) antenna without NL.

Table 1: MIMO antenna parameters values

Parameters	Value (mm)	Parameters	Value (mm)
h1	7.8	L1	16
h2	4	L2	16.5
h3	2.5	L3	4.75
h4	17	L4	6.75
h5	2.5	L5	5.25
h6	17	L6	5.75
h7	15	L7	1.5
h8	1	L8	2.6
		L9	7.25

The surface current distribution of the proposed antenna is used to analyse the contributions of the neutralization line properly. Two cases are studied at 2.4GHz, the first case is the proposed antenna with excluding neutralization line while the second case is the proposed antenna with including neutralization line. This study is performed by exciting port 1 and terminated port 2 with a matching load. Figure 2 demonstrates the surface current distribution with and without NL. It can be obviously seen that induced current in the feeding line port 2 is high in the case of the absence of the neutralization line. On the other hand, the existence of

the neutralization line will lead to introduce a new current path which generates an additional coupling to reduce the original coupling as shown in Fig. 2 (a) [36].

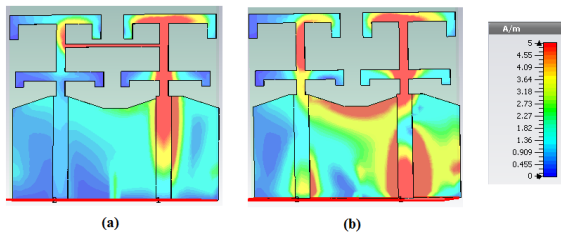


Fig. 2. Surface current distributions of the proposed MIMO antenna at 2.4GHz: (a) with NL and (b) without NL.

III. S-PARAMETERS OF THE PROPOSED ANTENNA WITH AND WITHOUT NL

The S-parameters of the antenna with and without the neutralization line are simulated to verify the effectiveness of the neutralization line (NL). Figure 3 shows the simulated result of the reflection coefficients S_{11} . It can be clearly observed that there is a shift to the right side (toward 2.4GHz) in the first band of operation and a reduction in the bandwidth of the same band. On the other hand, there is no effect on the second band after inserting the NL. Therefore, the same band is achieved.

The simulated coupling with and without NL is illustrated in Fig. 4. It can be clearly seen that the mutual coupling around 2.4GHz without NL is higher than -10dB. By inserting the neutralization line, the mutual coupling between the elements is decreased significantly in this band. The simulated isolation is nearly 27dB at 2.4GHz and 17dB at 5.5GHz as explained in Fig. 4.

IV. PARAMETRIC STUDY

To clarify the effects and obtain the optimized values of the proposed design, parametric studies based on the position and the width of the neutralization line were explained in Fig. 5 are carried out.

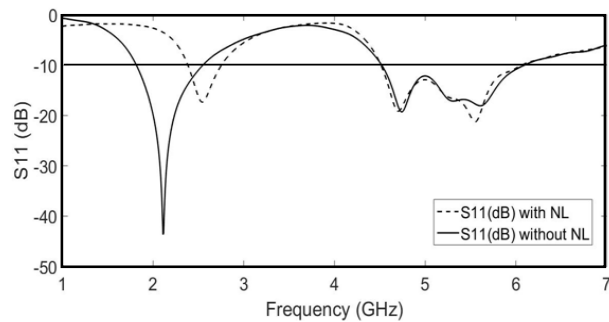


Fig. 3. Simulated reflection coefficients S_{11} with and without neutralization line for the proposed antenna.

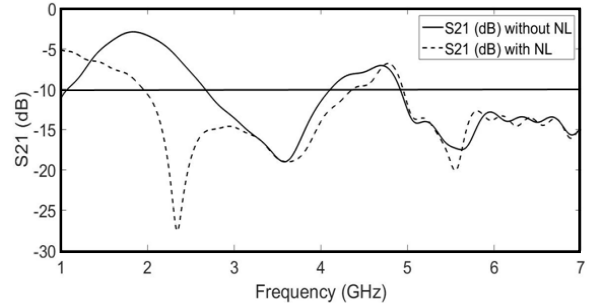


Fig. 4. Simulated transmission coefficients S_{21} with and without the neutralization line for the proposed antenna.

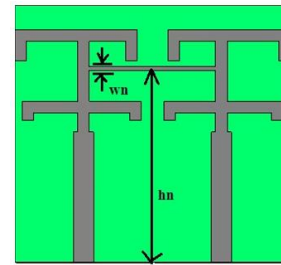


Fig. 5. Configuration of the proposed antenna for parametric study.

A. The effectiveness of the position of NL on the S-parameters

To validate the effectiveness of the position of the neutralization line, the simulated s-parameters of the antenna with different positions (h_n) of the NL are investigated as shown in Fig. 6 and Fig. 7 respectively. Figure 6 shows that by raising the position of the NL, the first band is shifted toward 2.4GHz band while the beginning of the second band is shifted backward. On the other hand, raising the position of the NL leads to decrease the mutual coupling between the elements in the first band and there are no effects on the second band. Tables 2 and 3 are summarized the values for the two figures to clarify the results.

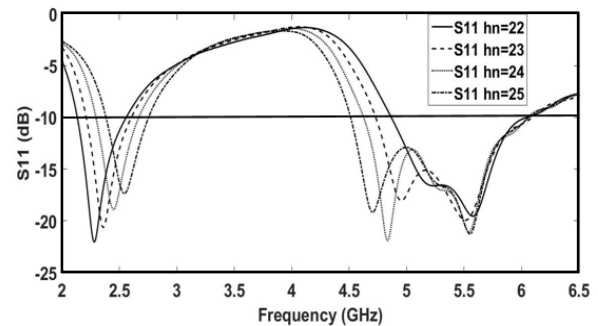


Fig. 6. The simulated reflection coefficient of the proposed antenna with different positions of NL.

Table 2: The effect of the position of NL on the reflection coefficients

	hn=22 mm	hn=23 mm	hn=24 mm	hn=25 mm
f=2.4 GHz	-11.1dB	-12.8dB	-16.7dB	-16.52dB
f=5.2 GHz	-16.58dB	-15.24dB	-15.8dB	-15.7dB
f=5.8 GHz	-13dB	-12.48dB	-12.29dB	-12.32dB

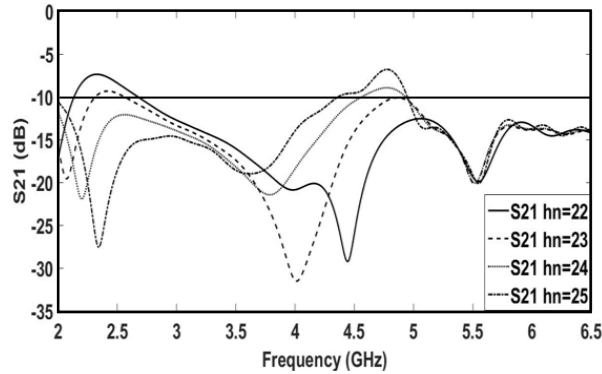


Fig. 7. Simulated transmission coefficient S21 of the third proposed antenna with different positions of NL.

Table 3: The effect of the position of NL on the transmission coefficients

	hn=22 mm	hn=23 mm	hn=24 mm	hn=25 mm
f=2.4 GHz	-8.3dB	-9.5dB	-12.2dB	-18.7dB
f=5.2 GHz	-13.19dB	-13.9dB	-13.99dB	-13.64dB
f=5.8 GHz	-13.76dB	-13.45dB	-13.28dB	-12.68dB

B. The effectiveness of the width of NL on the S-parameters of the proposed antenna

The width of the NL is changed from 0.25mm to 1mm, with 0.25mm steps. Figures 8 and 9 represent the reflection coefficients (S11) and the mutual coupling (S21) respectively. It can be clearly seen that by increasing the width of the NL, the reflection coefficients are decreased slightly and there are low effect on the two frequency bands. On the other hand, the mutual coupling values decrease by increasing the width of the NL at first band and there is a small effect on second band. The summarized values of the two figures are listed in Table 4 and Table 5 respectively.

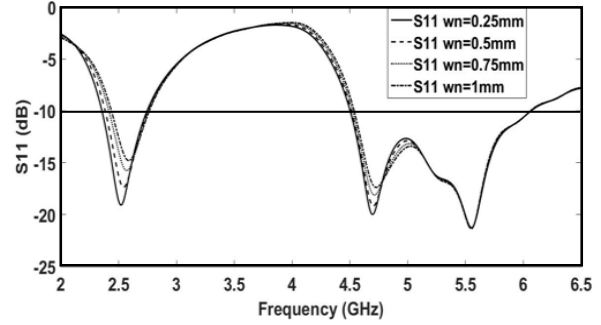


Fig. 8. Simulated reflection coefficient S11 of the third proposed antenna with different width of NL.

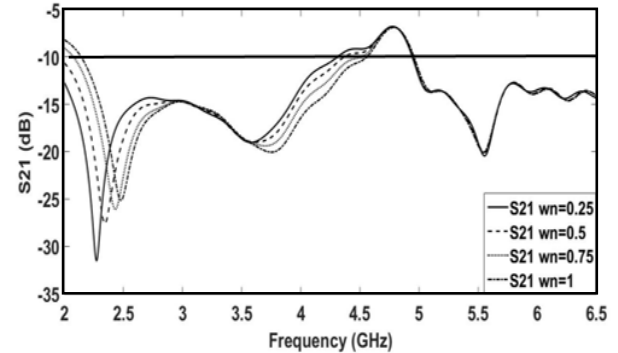


Fig. 9. Simulated transmission coefficient S21 of the third proposed antenna with different widths of NL.

Table 4: The effect of the width of NL on the reflection coefficients

	wn=0.25 mm	wn=0.5 mm	wn=0.75 mm	wn=1 mm
f=2.4 GHz	-18.7dB	-16.33dB	-13.9dB	-12.6dB
f=5.2 GHz	-15.7dB	-15.69dB	-15.6dB	-15.6dB
f=5.8 GHz	-12.32dB	-12.24dB	-12.1dB	-12.1dB

Table 5: The effect of the width of NL on the transmission coefficients

	wn=0.25 mm	wn=0.5 mm	wn=0.75 mm	wn=1 mm
f=2.4 GHz	-24 dB	-22.5 dB	-18.5dB	-16 dB
f=5.2 GHz	-13.7 dB	-13.66 dB	-13.68 dB	-13.7 dB
f=5.8 GHz	-12.8 dB	-12.7 dB	-12.7 dB	-12.7 dB

V. RESULTS AND DISCUSSION

To verify the simulated outcomes, the proposed

MIMO antenna is fabricated and tested. The prototype design of the proposed antenna is displayed in Fig. 10. The scattering parameters in terms of reflection coefficient (S_{11}) and transmission coefficient (S_{21}) were measured using vector network analyser (VNA) while the radiation patterns were measured facilities inside the anechoic chamber. Distinguishing features such as high isolation between the radiating elements, low values for envelope correlation coefficient and channel capacity loss, TARC value $\leq -10\text{dB}$ within the desired frequency band and omnidirectional radiation pattern, indicate the potential of proposed MIMO antenna. The designed antenna was prototyped using the same substrate and dimensions used in the simulation. The comparisons between the simulated and the measured results in terms of S-parameters are plotted in Fig. 11 and Fig. 12 respectively. It can be clearly seen that there is a reasonable agreement between results with some tolerance that can be attributed to reflections from the SMA connectors and the objects near the antenna during the tests. The measured impedance bandwidths of the antenna cover the operating frequency bands from 2.4 to 2.7GHz and from 4.4 GHz to 6.7GHz for the reflection coefficient $|S_{11}| \leq -10\text{dB}$. These achieved bandwidths fulfil the requirements of the WLAN applications. On the other hand, the result of S_{21} for the two bands is less than -10dB and it reaches to -30dB around 2.4 GHz and 5.5GHz.

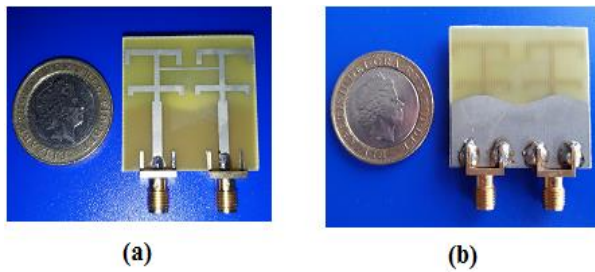


Fig. 10. The fabricated MIMO antenna design with N: (a) top view and (b) back view.

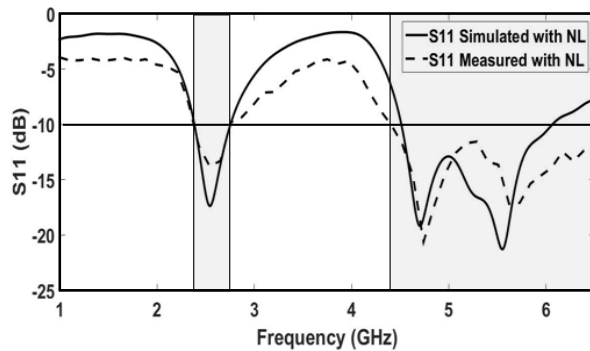


Fig. 11. Simulated and measured S_{11} of the proposed MIMO antenna with NL.

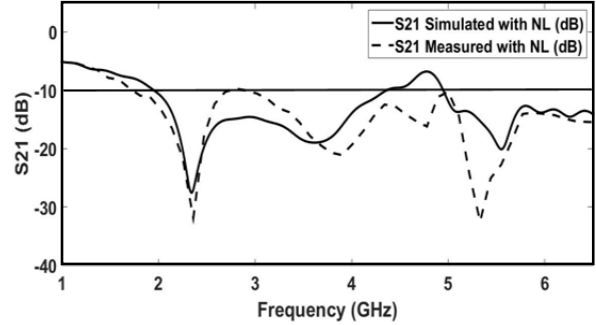


Fig. 12. Simulated and measured S_{21} of the proposed MIMO antenna with parasitic elements.

Generally, the envelope correlation coefficient (ECC) is a significant factor in MIMO antenna systems due to its ability to examine how much the radiating elements are independent and they rely on their individual performances. The evaluation of the ECC of a MIMO antenna could be obtained through two different approaches. The first method depends on the far-field radiation pattern of the antenna [1, 37] and the second method uses the S-parameters of the antenna [30]. The simulated and measured ECC of the proposed MIMO antenna were calculated using equation 1 [30] and the results are illustrated in Fig. 13. It can be clearly seen from Fig. 13 that the value of the ECC is less than 0.025 in two bands which is significantly less than the 0.3, the requirement for MIMO antenna applications [28]:

$$ECC = \frac{|S_{11}^* S_{12} + S_{21}^* S_{22}|}{(1 - |S_{11}|^2 - |S_{21}|^2)(1 - |S_{22}|^2 - |S_{12}|^2)} \quad (1)$$

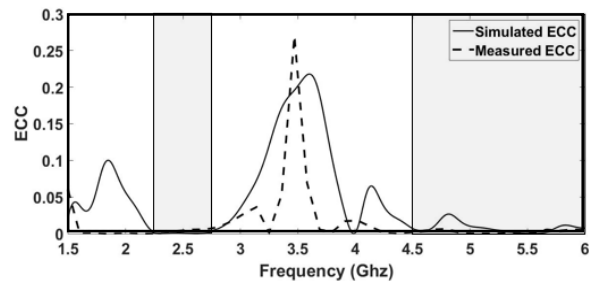


Fig. 13. Simulated and measured ECC of the proposed MIMO antenna with NL.

Basically, the channel capacity of the MIMO system could be improved by increasing the number of antennas. whilst the existence of the uncorrelated Rayleigh-fading may lead to a loss in the channel capacity. For two elements of MIMO systems, the channel capacity loss could be calculated by using the correlation matrix mentioned in [38]. The simplified form of channel capacity loss is listed below [39]:

$$C_{loss} = -\log_2 \det(\varphi^R), \quad (2)$$

where φ^R is the correlation matrix receiving antenna:

$$\varphi^R = \begin{bmatrix} \rho_{11} & \rho_{12} \\ \rho_{21} & \rho_{22} \end{bmatrix},$$

$$\text{with } \rho_{ii} = \left(1 - (|S_{ii}|^2 + |S_{ij}|^2)\right),$$

$$\text{and } \rho_{ij} = -(S_{ii}^* S_{ij} + S_{ji}^* S_{jj}) \quad i, j = 1 \text{ or } 2.$$

The computed and measured capacity loss of the proposed MIMO antenna is illustrated in Fig. 14. In this figure, the capacity loss is less than 1 bit/s/Hz for the two bands and there is a very good agreement between the calculated and measured results.

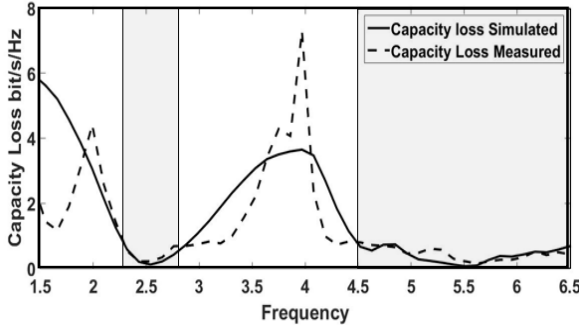


Fig. 14. Simulated and measured CCL of the proposed MIMO antenna with parasitic elements.

The total active reflection coefficient (TARC) is a considerable parameter in the MIMO antenna system which is used to properly characterize the bandwidth and efficiency of the system. TARC defines as the result of dividing the square root of the total reflected power to the square root of the total incident power [28]. Equation (3) uses to evaluate the TARC value in the two-port MIMO antenna system [14]:

$$\tau_a^t = \sqrt{\frac{(|S_{11} + S_{12}e^{j\theta}|^2) + (|S_{21} + S_{22}e^{j\theta}|^2)}{2}}. \quad (3)$$

The computed TARC of the present design is explained in Fig. 15 and Fig. 16 respectively. Figure 15 is created using equation (3) to cover the phase range from 0 to 180 degrees with phase steps of 30 degrees. The average value of TARC is shown in Fig. 16. It can be clearly seen that the two bands appeared with a TARC value of less than -10dB.

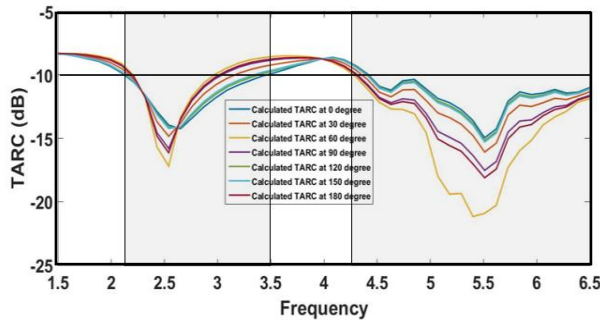


Fig. 15. Calculated TARC with a different phase of the proposed MIMO antenna with parasitic elements.

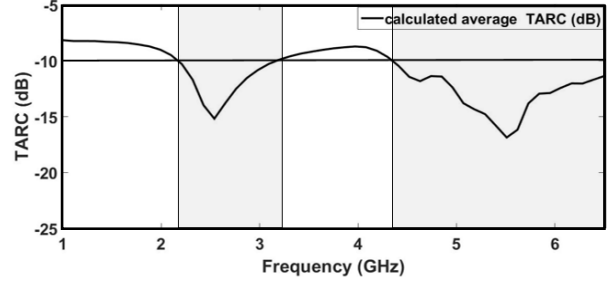


Fig. 16. The calculated average value of TARC for the proposed MIMO antenna with parasitic elements.

Diversity Gain (DG) is another important factor that affects the performance of a MIMO antenna system. This metric can be defined as the amount of improvement in the diversity antenna system compared to a single antenna system in one diversity channel [28]. In this paper, the DG can be calculated using the following equation [40]:

$$DG = 10\sqrt{1 - (ECC)^2}. \quad (4)$$

Figure 17 represents the simulated DG of the proposed MIMO antenna. It can be clearly seen that the DSs values for the two frequency bands are very close to the ideal value of DG (DG=10dB).

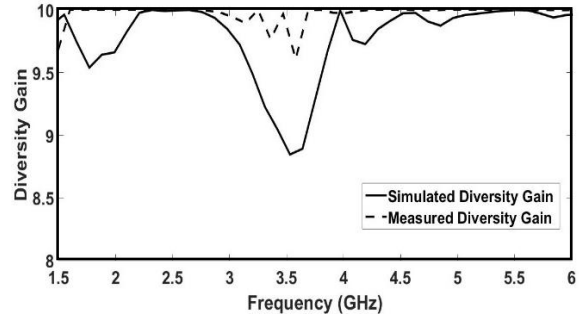


Fig. 17. The simulated and measured diversity gain of the proposed MIMO antenna.

Finally, the prototyped design of the proposed antenna is tested in terms of far-field radiation patterns at three different frequencies in the anechoic chamber of the University of Bradford. These patterns were measured in the two planes of XZ and YZ, in the case of exciting port 1 and terminating port 2. The elevation-over-azimuth positioner was used by synchronizing the elevation axis with the MIMO antenna's coordinate system at ($\theta = 0^\circ$). Therefore, cuts at constant ϕ will be generated by the azimuth drive. A broadband horn (EMCO type 3115) is used as a transmitting antenna and a 4m distance was kept between the transmitter and the antenna under test. The measurements have carried out by rotating the azimuth positioner from $\theta = -180$ to 180 at increments of 5 degrees. The practical results are shown in Fig. 18 and they explain that at the three

frequencies, the far-field radiations achieve stable omnidirectional patterns. For further evaluation of the volumetric radiation patterns, the three-dimensional variation of the radiated field for the proposed antenna is calculated at three frequencies and are shown in Fig. 19. This figure gives more appreciation of the field shape as compared to that of the 2-D representations.

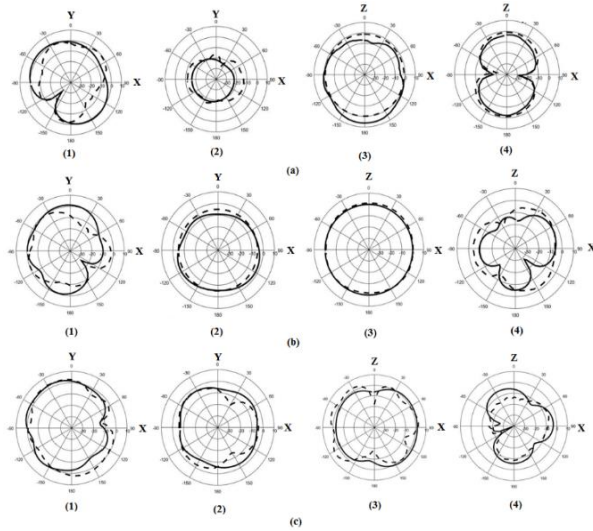


Fig. 18. Simulated and measured radiation patterns of the proposed antenna for two planes [(1 and 2) y-x plane and (3 and 4) z-x plane] at: (a) 2.4GHz, (b) 5.2GHz, and (c) 5.8GHz. Port 1 is excited and port 2 is terminated. “—” simulated results, “- - -” measured results, ‘1 and 3’ co-polar components and “2 and 4” cross-polar components.

VI. COMPARISON WITH PUBLISHED WORKS

Furthermore, the proposed MIMO antenna is compared with several published data from other researchers. All the antennas in this comparison were used neutralization line as reduction technique in their antennas. This comparison is not comprehensive, but it has a fair representative for the state of the art of this technology. The comparison depends on the overall size of the antenna, the frequency of operation, the separation distance between the radiating elements, the isolation between the elements and the diversity performance in terms of ECC, CCL, TARC and DG. The summary of this comparison has listed in Table 6. It can be noticed that the dimensions of the proposed antenna are moderate between the other antennas. The isolation of the proposed antenna is shown to provide a good value compared to the distance between the radiating elements. Low-level correlation coefficient and minimum channel capacity loss compared with other designs have also been obtained. These features confirm that this design is a good candidate for the MIMO antenna design.

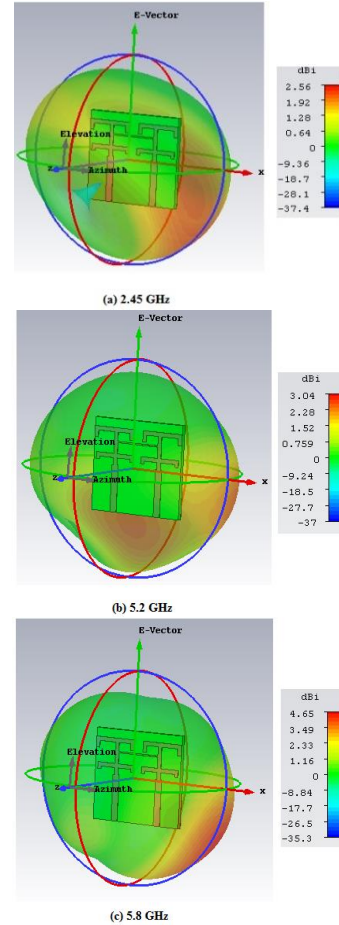


Fig. 19. The simulated 3-D pattern of the proposed MIMO antenna at: (a) 2.4GHz, (b) 5.2GHz, and (c) 5.8GHz.

Table 6: Comparison with other works

Ref. No.	41	42	43	44
Size (mm ³)	26.7x32.94x1.6	60x7.5x4.5	40x90x0.79	35x16x0.8
BW (GHz)	3.05-13.5	2.4-2.484 5.15-5.85	2.4-4.2	3.1-5
Separation distance	0.52mm	18mm	18.8mm	2.2mm
Isolation (dB)	≥10	Max 16, 23	≥16	Max 22
ECC	≤0.1	NA	≤0.06	NA
CCL (bps/s/Hz)	NA	NA	NA	NA
TARC≤-10dB	NA	NA	NA	NA
DG (dB)	NA	NA	NA	NA
Ref. No.	45	46	47	This Antenna
Size (mm ³)	120x60x0.8	80x60x0.8	65x30x1	36x33.5x1.6
BW (GHz)	0.76-0.82	1.67-2.76	2.38-2.51	2.42.7 4.4-6.7
Separation distance	10mm	10mm	14mm	3mm
Isolation (dB)	Max 11.5	≥15	Max 22	≥15
ECC	≤0.5	≤0.05	≤0.006	≤0.1
CCL (bps/s/Hz)	NA	NA	NA	≤0.05
TARC≤-10dB	NA	NA	Cover the band	Covers the two bands
DG (dB)	NA	≥9.98	NA	≥9.99

VII. CONCLUSION AND FUTURE WORK

A compact dual-band MIMO antenna operating at WLAN bands (2.4/5.2/5.8 GHz) has been designed. The schematic structure of this antenna consists of two double T-shaped radiating elements with a neutralization line to connect them. The optimum value of isolation has been obtained by optimizing the neutralization line in terms of width and position. The antenna has achieved bandwidths from 2.4GHz to 2.7GHz and from 4.4 to 6.7 for reflection coefficient $|S_{11}| \leq -10\text{dB}$. On the other hand, the results of S_{21} for the two bands are better than -15dB and it has reached to -30dB around 2.4GHz and 5.5GHz. The Envelope correlation coefficient has also been evaluated and found to be less than 0.01 in the two bands. Channel capacity loss is another parameter that has been calculated and presented. The obtained value of CCL is less than 0.5 bps/s/Hz in the two required bands. The simulated and measured average TARCs have been also illustrated. It has been observed that the two bands appeared with a TARC value of less than -10dB . Diversity gain is another important metric that has been studied in this work. The achieved value of DG is very close to the ideal value (10dB) over the two frequency bands. The simulated and measured radiation patterns were presented at three different frequencies and they showed nearly a stable omnidirectional behavior. These achievements indicate that the proposed antenna can be a good candidate to work within WLAN frequency band applications. Some differences have been noticed between the simulated and measured results which related to manufacturing and measurement tolerances. Finally, an interesting area of using a Genetic Algorithm (GA) to evaluate the effect of neutralization lines within the MIMO antenna structure can be used to extend this work in the future.

ACKNOWLEDGEMENTS

Adham M. Saleh would like to thank the Higher Committee for Education Development in Iraq (HCED) for supporting this project financially and monitoring his Ph.D. progress. The authors would like to acknowledge Ninevah University and the University of Bradford for their massive support during this project.

REFERENCES

- [1] R. G. Vaughan and J. B. Andersen, "Antenna diversity in mobile communications," *IEEE Transactions on Vehicular Technology*, vol. VT-36, pp. 147-172, Nov. 1987.
- [2] G. J. Foschini and M. J. Gans, "On limits of wireless communications in a fading environment when using multiple antennas," *Wireless Pers. Commun.*, vol. 6, pp. 311-335, 1998.
- [3] J. Leivo, "Improving the performance of strongly coupled antennas using a compensating transmission line network," *M.Sc. Thesis*, Gothenburg, Chalmers University of Technology, Sweden, 2009.
- [4] S. R. Saunders and A. A. Zavala, *Antennas and Propagation for Wireless Communication Systems*, 2nd Ed., John Wiley & Sons Ltd, 2007.
- [5] C. H. See, et al., *Compact Wideband Printed MIMO/Diversity Monopole Antenna for GSM/UMTS and LTE Applications*. In: I. Elfergani, A. Hussaini, J. Rodriguez, R. Abd-Alhameed (eds), *Antenna Fundamentals for Legacy Mobile Applications and Beyond*. Springer, Cham, 2018.
- [6] R. Addaci, A. Diallo, C. Luxey, P. Le Thuc, and R. Staraj, "Dual-band WLAN diversity antenna system with high port-to-port isolation," in *IEEE Antennas and Wireless Propagation Letters*, vol. 11, pp. 244-247, 2012.
- [7] X. B. Sun and M. Y. Cao, "Low mutual coupling antenna array for WLAN application," in *Electronics Letters*, vol. 53, no. 6, pp. 368-370, 2017.
- [8] X. L. Liu, Z. Wang, Y.-Z. Yin, and J. H. Wang, "Closely spaced dual band-notched UWB antenna for MIMO applications," *Progress In Electromagnetics Research C*, vol. 46, pp. 109-116, 2014.
- [9] H. Qin and Y.-F. Liu, "Compact dual-band MIMO antenna with high port isolation for WLAN applications," *Progress In Electromagnetics Research C*, vol. 49, pp. 97-104, 2014.
- [10] P. Sharma and T. Khanb, "A compact MIMO antenna with DGS structure," *International Journal of Current Engineering and Technology*, vol. 3, no. 3, pp. 780-782, 2013.
- [11] W. N. N. W. Marzudi, et al., "Uni-planer MIMO antenna for WLAN and WiMAX wireless services," *International Journal of Computer and Information Technology*, vol. 8, no. 3, pp. 78-83, May 2019.
- [12] H. Zhao, F. Zhang, C. Wang, and J. Liang, "A compact UWB diversity antenna," *International Journal of Antennas and Propagation*, vol. 2014, Article ID 805853, 6 pages, 2014.
- [13] W. N. N. W. Marzudi, et al., *Two-Elements Crescent Shaped Printed Antenna for Wireless Applications*. In: H. Sulaiman, M. Othman, M. Othman, Y. Rahim, N. Pee (eds), *Advanced Computer and Communication Engineering Technology. Lecture Notes in Electrical Engineering*, vol. 315, Springer, Cham, 2015.
- [14] S. Su, C. Lee, and F. Chang, "Printed MIMO-antenna system using neutralization-line technique for wireless USB-dongle applications," in *IEEE Transactions on Antennas and Propagation*, vol. 60, no. 2, pp. 456-463, Feb. 2012.
- [15] Y. Wang and Z. Du, "A wideband printed dual-antenna with three neutralization lines for mobile terminals," in *IEEE Transactions on Antennas and Propagation*, vol. 62, no. 3, pp. 1495-1500, Mar. 2014.
- [16] S. Zhang and G. F. Pedersen, "Mutual coupling reduction for UWB MIMO antennas with a

- wideband neutralization line,” in *IEEE Antennas and Wireless Propagation Letters*, vol. 15, pp. 166-169, 2016.
- [17] A. M. Saleh, K. H. Sayidmarie, R. A. Abd-Alhameed, S. Jones, J. M. Noras, and P. S. Excell, “Compact tri-band MIMO antenna with high port isolation for WLAN and WiMAX applications,” *2016 Loughborough Antennas & Propagation Conference (LAPC)*, Loughborough, pp. 1-4, 2016.
- [18] R. Selvaraju, M. H. Jamaluddin, M. R. Kamarudin, J. Nasir, and M. H. Dahri, “Complementary split ring resonator for isolation enhancement in 5G communication antenna array,” *Prog. Electromagn. Res.*, vol. 83, pp. 217-228, 2018.
- [19] M. M. Bait-Suwailam, O. F. Siddiqui, and O. M. Ramahi, “Mutual coupling reduction between microstrip patch antennas using slotted-complementary split-ring resonators,” in *IEEE Antennas and Wireless Propagation Letters*, vol. 9, pp. 876-878, 2010.
- [20] Z. Qamar, L. Riaz, M. Chongcheawchamnan, S. A. Khan, and M. F. Shafique, “Slot combined complementary split-ring resonators for mutual coupling suppression in microstrip phased arrays,” in *IET Microwaves, Antennas & Propagation*, vol. 8, no. 15, pp. 1261-1267, 9 12 2014.
- [21] M. S. Sharawi, M. U. Khan, A. B. Numan, and D. N. Aloï, “A CSRR loaded MIMO antenna system for ISM band operation,” in *IEEE Transactions on Antennas and Propagation*, vol. 61, no. 8, pp. 4265-4274, Aug. 2013.
- [22] A. Ramachandran, S. Valiyaveetil Pushpakaran, M. Pezholil, and V. Kesavath, “A four-port MIMO antenna using concentric square-ring patches loaded with CSRR for high isolation,” in *IEEE Antennas and Wireless Propagation Letters*, vol. 15, pp. 1196-1199, 2016.
- [23] M. S. Khan, A. Capobianco, S. M. Asif, D. E. Anagnostou, R. M. Shubair, and B. D. Braaten, “A compact CSRR-enabled UWB diversity antenna,” in *IEEE Antennas and Wireless Propagation Letters*, vol. 16, pp. 808-812, 2017.
- [24] W. T. Li, Y. Q. Hei, H. Subbaraman, X. W. Shi, and R. T. Chen, “Novel printed filtenna with dual notches and good out-of-band characteristics for UWB-MIMO applications,” in *IEEE Microwave and Wireless Components Letters*, vol. 26, no. 10, pp. 765-767, Oct. 2016.
- [25] D. A. Ketzaki and T. V. Yioultis, “Metamaterial-based design of planar compact MIMO monopoles,” in *IEEE Transactions on Antennas and Propagation*, vol. 61, no. 5, pp. 2758-2766, May 2013.
- [26] M. G. N. Alsath, M. Kanagasabai, and B. Balasubramanian, “Implementation of slotted meander-line resonators for isolation enhancement in microstrip patch antenna arrays,” *IEEE Antennas and Wireless Propagation Letters*, vol. 12, pp. 15-18, 2013.
- [27] I. Nadeem and D. Choi, “Study on mutual Coupling reduction technique for MIMO antennas,” in *IEEE Access*, vol. 7, pp. 563-586, 2019.
- [28] M. R. Sharawi, *Printed MIMO Antenna Engineering*. Norwood: Artech House, 2014.
- [29] J. Byun, J.-H. Jo, and B. Lee, “Compact dual-band diversity antenna for mobile handset applications,” *Microwave and Optical Technology Letters*, vol. 50, pp. 2600-2604, 2008.
- [30] K. Chung and J. H. Yoon, “Integrated MIMO antenna with high isolation characteristic,” *Electronics Letters*, vol. 43, pp. 199-201, 2007.
- [31] S.-W. Su, C.-T. Lee, and F.-S. Chang, “Printed MIMO-antenna system using neutralization-line technique for wireless USB-dongle applications,” *IEEE Transactions. Antennas Propagation*, vol. 60, no. 2, pp. 456-463, Feb. 2012.
- [32] S. Wang and Z. Du, “Decoupled dual-antenna system using crossed neutralization lines for LTE/WWAN smartphone applications,” in *IEEE Antennas and Wireless Propagation Letters*, vol. 14, pp. 523-526, 2015.
- [33] Y. Ou, X. Cai, and K. Qian, “Two-element compact antennas decoupled with a simple neutralization line,” *Prog. Electromagn. Res.*, vol. 65, pp. 63-68, 2017.
- [34] W. A. E. Ali and A. A. Ibrahim, “A compact double-sided MIMO antenna with an improved isolation for UWB applications,” *AEU-Int. J. Electron. Commun.*, vol. 82, pp. 7-13, Dec. 2017.
- [35] S. Papantonis and E. Episkopou, “Compact dual-band printed 2.5-shaped monopole antenna for WLAN applications,” *Progress In Electromagnetics Research C*, vol. 24, pp. 57-68, 2011.
- [36] Y. Ban, Z. Chen, Z. Chen, K. Kang, and J. L. Li, “Decoupled hepta-band antenna array for WWAN/LTE smartphone applications,” in *IEEE Antennas and Wireless Propagation Letters*, vol. 13, pp. 999-1002, 2014.
- [37] R. A. Bhatti, J. Choi, and S. Park, “Quad-band MIMO antenna array for portable wireless communications terminals,” in *IEEE Antennas and Wireless Propagation Letters*, vol. 8, pp. 129-132, 2009.
- [38] S. H. Chae, S. Oh, and S. Park, “Analysis of mutual coupling, correlations, and TARC in WiBro MIMO array antenna,” in *IEEE Antennas and Wireless Propagation Letters*, vol. 6, pp. 122-125, 2007.
- [39] C. H. See, R. A. Abd-Alhameed, Z. Z. Abidin, N. J. McEwan, and P. S. Excell, “Wideband printed MIMO/diversity monopole antenna for WiFi/WiMAX applications,” in *IEEE Transactions on Antennas and Propagation*, vol. 60, no. 4, pp. 2028-2035, Apr. 2012.
- [40] A. Kumar, et al., “High isolation compact four-port MIMO antenna loaded with CSRR for multiband

applications," *Frequenz*, 72.9-10, pp. 415-427, 2018. Retrieved 12 Aug. 2019, from doi:10.1515/freq-2017-0276.

- [41] J. Banerjee, R. Ghatak, and A. Karmakar, "A compact planar UWB MIMO diversity antenna with Hilbert fractal neutralization line for isolation improvement and dual band notch characteristics," *2018 Emerging Trends in Electronic Devices and Computational Techniques (EDCT)*, Kolkata, pp. 1-6, 2018.
- [42] C. Jui-Hung, et al., "Dual-band WLAN MIMO antenna with a decoupling element for full-metallic bottom cover tablet computer applications," *Microwave and Optical Technology Letters*, vol. 60, no. 5, pp. 1245-1251, 2018.
- [43] E. Elkazmi, C. H. See, N. A. Jan, R. A. Abd-Alhameed, N. Ali, and N. J. McEwan, "Design of a wideband printed MIMO monopole antenna using neutralization lines technique," *Asia-Pacific Microwave Conference*, Sendai, Japan, pp. 983-985, 2014.
- [44] S. Zhang and G. F. Pedersen, "Mutual coupling reduction for UWB MIMO antennas with a wideband neutralization line," in *IEEE Antennas and Wireless Propagation Letters*, vol. 15, pp. 166-169, 2016.
- [45] A. Cihangir, F. Ferrero, G. Jacquemod, P. Brachat, and C. Luxey, "Neutralized coupling elements for MIMO operation in 4G mobile terminals," in *IEEE Antennas and Wireless Propagation Letters*, vol. 13, pp. 141-144, 2014.
- [46] Y. Wang and Z. Du, "A wideband printed dual-antenna system with a novel neutralization line for mobile terminals," in *IEEE Antennas and Wireless Propagation Letters*, vol. 12, pp. 1428-1431, 2013.
- [47] S. Su, C. Lee, and F. Chang, "Printed MIMO-antenna system using neutralization-line technique for wireless USB-dongle applications," in *IEEE Transactions on Antennas and Propagation*, vol. 60, no. 2, pp. 456-463, Feb. 2012.

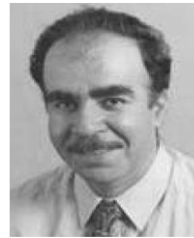


Adham Maan Saleh was born in Mosul, Iraq, in 1984. He received the B.Sc. and M.Sc. degrees from Ninevah University, Iraq in 2006 and 2012, respectively, all in Communications Engineering. Currently, he is working toward the Ph.D. degree from the School of Engineering and Informatics, Bradford University, West Yorkshire, UK. He was a Lecturer at Ninevah University since 2012. His current research interests include MIMO antenna design, defected ground structures (DGS), neutralization

techniques for wireless and mobile systems, reflectarray antennas, and multiband antennas techniques.



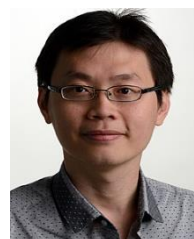
Tariq A. Nagem was born in Mosul, Iraq, in 1984. He received the B.Sc. and M.Sc. degrees from Ninevah University, Iraq in 2006 and 2013, respectively, all in Communications Engineering. He was a Lecturer at Ninevah University since 2013. His current research interests include MIMO antenna design, filters design, ultra-wide band antennas (UWB) and multi-band antenna techniques.



Raed A. Abd-Alhameed received the B.Sc. and M.Sc. degrees from Basrah University, Basrah, Iraq, in 1982 and 1985, respectively, and the Ph.D. degree from the University of Bradford, West Yorkshire, U.K., in 1997, all in Electrical Engineering. He is a Professor of electromagnetic and radio frequency engineering at the University of Bradford. He is the senior academic responsible for electromagnetics research in the Mobile and Satellite Communications Research Center, University of Bradford.



James M. Noras received the B.Sc. degree in Physics and the Ph.D. degree in Semiconductor Physics from St. Andrews University, Scotland, in 1973 and 1978, respectively, and the M.Sc. degree in Mathematics from the Open University, U.K., in 1995. He is a Senior Lecturer in the School of Engineering, Design and Technology at the University of Bradford, UK. He is the Director of five internationally franchised B.Eng. and M.Sc. courses in Electrical and Electronic Engineering has successfully supervised 18 Ph.D. students and is currently supervising the research of three Ph.D. students. His main research interests are now in digital system design and implementation, DSP and coding for communication systems, and localization algorithms for mobile systems.



Chan H. See received a first-class B.Eng. Honours degree in Electronic, Telecommunication and Computer Engineering and a Ph.D. degree from the University of Bradford, UK. Since 2019, He has been appointed as Associate Professor within the School of Engineering and the Built Environment, Edinburgh Napier University. See is a

Chartered Engineer and Fellow of the Institution of Engineering and Technology (FIET) and Senior Member of Institute of Electrical and Electronics Engineers

(SMIEEE). He has an NVQ level 4 in Management from the Chartered Management Institute.